Polymer(Korea), Vol. 38, No. 6, pp. 726-734
http://dx.doi.org/10.7317/pk.2014.38.6.726

ISSN 0379-153X(Print)
ISSN 2234-8077(Online)

유리섬유강화 에폭시 레진 복합체의 기계적, 유전체 특성에 미치는 첨가제 함유 에폭시 영향

Cuong Manh Vu†, Liem Thanh Nguyen*, Thai Viet Nguyen, 최형진**,†
Chemical Deparment, Le Qui Don Technical University,
*Polymer Center, Ha Noi University of Science and Technology, ** 인하대학교 고분자공학과
(2014년 3월 22일 접수, 2014년 4월 27일 수정, 2014년 4월 28일 채택)

Effect of Additive-added Epoxy on Mechanical and Dielectric Characteristics of Glass Fiber Reinforced Epoxy Composites

Cuong Manh Vu†, Liem Thanh Nguyen*, Thai Viet Nguyen, and Hyoung Jin Choi,†**

Chemical Deparment, Le Qui Don Technical University, No. 236 Hoang Quoc Viet, Ha Noi, Viet Nam
**Polymer Center, Ha Noi University of Science and Technology, No.1, Dai Co Viet, Ha Noi, Viet Nam*
***Department of Polymer Science and Engineering, Inha University, Incheon 402-751, Korea*
(Received March 22, 2014; Revised April 27, 2014; Accepted April 28, 2014)

Abstract: Three different types of additives, thiokol, epoxidized natural rubber (ENR) and epoxidized linseed oil (ELO), were dispersed in an epoxy matrix before being used in glass fiber (GF) composites, and their effects on the mechanical and dielectric properties of epoxy resin and glass fiber reinforced epoxy composites (GF/EP) were examined. The addition of each of 7 phr ENR, 9 phr ELO and 5 phr thiokol into the epoxy resin increased the fracture toughness significantly by 56.9, 43.1, and 80.0%, respectively, compared to the unmodified resin. The mode I interlaminar fracture toughness of the GF/EP at propagation was also improved by 26.9, 18.3 and 32.7% when each of 7 phr ENR, 9 phr ELO, and 5 phr thiokol, respectively, was dispersed in the epoxy matrix. Scanning electron microscopy showed that the additives reduced crack growth in the GF/EP, whereas their dielectric measurements showed that all these additives had no additional effect on the real permittivity and loss factor of the GF/EP.

Keywords: glass fiber, epoxy resin, fracture toughness, dielectric property.

Introduction

Fiber reinforced composites are used widely in the fields of space, aircraft, automobile and sports industries because of their high strength and stiffness to weight ratios. On the other hand, it is essential to examine the resistance against delamination propagation, which is useful in the design and analysis of composite structures because one of the limitations of these materials is their poor ability to resist impact and delamination.[1]

The strength properties of glass fiber reinforced epoxy composites (GF/EP) are sensitive to the failure modes, such as transverse cracking, longitudinal cracking and delamination between the adjacent layers, due to the intrinsic brittleness of the epoxy matrix. Recent studies showed that most failure modes of GF/EP could be controlled gradually. Epoxies are used widely as a polymer matrix for high performance laminated composites because of their good mechanical performance, processability, and compatibility to most fibers with chemical resistance, wear resistance and low cost. These materials, however, are relatively brittle after curing, which is detrimental to the interlaminar properties. Therefore, substantial efforts have been made towards improving the fracture toughness by toughening the matrix material. Their mechanical performance would be enhanced dramatically by incorporating a small amount of nano-materials, such as carbon nanotube, nano-clay, nano-cellulose, and nano-thermoplastic fibers or micro-fillers to the epoxy matrix,[2] whereas it has been reported that epoxy with smaller size fillers has better fracture performance than that with larger-size fillers.[3-5]

The toughening effect of nano-filler on the GF/EP was also examined.[6-10] Recently, Liu *et al.*[11] carried out a systematic

†To whom correspondence should be addressed.
E-mail: vumanhcuong309@gmail.com; hjchoi@inha.ac.kr

study on the toughening of bulk epoxy using nano-silica, nano-rubber and nano-silica/nano-rubber particles. Compared to the nano-silica particles, nano-rubber was found to have a more significant effect on the toughness. The Mode I fracture toughness of the rubber-modified epoxy increased with increasing particle loading up to 15 wt%, but the Young's modulus of the composite reduced to 78% of the neat epoxy. The fracture toughness of the hybrid nano-silica and nano-rubber particles in the epoxy had no synergistic effect other than the sum of the toughness value due to each nano-particle.[11]

Liquid rubber, such as carboxyl-terminated butadiene acrylonitrile (CTBN) rubber, has potential as a modifier for GF/EP without changing the viscosity.[12,13] When this system is cured, the epoxy polymerizes and CTBN reacts with the epoxy to form a copolymer. With increasing molecular weight, the soluble reactive liquid CTBN rubber phase separates from the epoxy because of the decrease in rubber/epoxy compatibility. The elastomeric phase forms small discrete particles, typically in the micrometer range, which are dispersed in and bonded to the epoxy matrix. Although the morphology of rubber in toughened epoxy systems is mostly spherical, the mean particle size and distribution can vary considerably, depending on the curing reactions, cure cycle and concentration of rubber in the epoxy system.[14-17] Abadyan *et al*.[18] examined the rubber modification of hoop filament wound epoxy composites using amine-terminated butadiene acrylonitrile (ATBN) and CTBN oligomers for two different hybrid modified epoxies. In one system, the epoxy was modified by ATBN and hollow glass spheres as fine and coarse modifiers, respectively. The other hybrid epoxy was modified by a combination of ATBN and recycled tire particles. The measured fracture toughness of the blends revealed synergistic toughening for both hybrid systems in some formulations.[19]

The fracture toughness of resins modified with liquid rubber increased with increasing CTBN content up to 17%. The maximum fracture toughness of the modified epoxy was approximately 30 times that of the unmodified epoxy, whereas the fracture toughness of vinylester resin modified with CTBN was approximately four times that without modification. The CTBN modifier also increased the ductility by almost 100% at the expense of concomitant reductions in strength and modulus. Despite the large increase in fracture toughness of the bulk resin, the same increase was not guaranteed when the modified resin was used as an adhesive or as a matrix material for fiber-reinforced composites up to 200% improvements in interlaminar fracture toughness was reported for carbon fiber-CTBN-modified epoxy matrix composites.[20]

On the other hand, to design unmanned aerial vehicles, there is a demand for radio frequency transparency. Therefore, it is essential to understand both mechanical properties and dielectric properties of GF/EP. The dielectric properties of GF/EP in the centimeter wave range (8.2-12.4 GHz) were measured using the free-space method reported by Seo *et al*..[21]

This study examined the production and characterization of epoxidized natural rubber (ENR), epoxidized linseed oil (ELO), and thiokol-modified glass fiber/epoxy laminated composites. An epoxy system already optimized for toughness through the incorporation of conventional modifiers was chosen as the baseline material. The mechanical properties of the modified epoxy resin containing different ENR, ELO, and thiokol contents were compared with the unmodified epoxy resin. Based on these results, GF/EP made of 7 phr ENR, 9 phr ELO, and 5 phr thiokol modified epoxy resin were manufactured to determine the mechanical and dielectric properties, including tensile strength, Mode I interlaminar fracture toughness, and dielectric constant.

Experimental

Materials. The epoxy resin (EP) used in all experiments was diglycidal ether of bisphenol A (DER 331, Dow Chemical Co.), and dietylentriamine (DETA) (Dow Chemical Co.) was used as a curing agent. The ENR of Figure 1 (epoxide percentage: 50%, M_n=10000-20000 g/mol), supplied by the Vietnamese Military Institute of Science and Technology, was prepared by reacting the natural rubber latex (NR) of *cis*-1,4-isoprene with performic acid (product of reaction between formic acid and hydrogen peroxide), as shown in Figure 2. The ELO (viscous liquid, light yellow color, epoxide percentage: 21.6%, iodine value: 2, 4 g of I_2/g, acid value: 0.5 mg KOH/g, density at 20 °C: 1-1.2 g/cm^3 and boiling point is higher than 200 °C) was purchased from Akcros Chemicals (UK). Thiokol was Thioplast G21 from Akazo Nobel. The woven roving E-glass fiber with area weight of 300 g/m^2 (WRE300) was purchased from Jiujiang Beihai Fiberglass Co., China.

Preparation of Samples. Solutions of each additive of ENR (5-20 phr), ELO (5-20 phr) and thiokol (3-9 phr) with different concentrations in the epoxy resin were first mixed together using a mechanical stirrer, and heated for 1 h at around 60 °C in a water bath to ensure proper dispersion of the additive. The mixtures were cooled to room temperature, while a curing agent was added prior to hand mixing for approx-

imately 20 min. The products were degassed using a vacuum pump. Next, the resin mixture was poured into a 4 mm-thick mould that was coated with a release agent. The samples were pre-cured at room temperature for 24 h and then post-cured at 80 ºC for 3 h. At this stage the cured specimens were allowed to cool slowly at room temperature. Once all formulations were made, they were then reinforced with hand layup glass fiber process to form composite sheets. They were finally cured at the same temperature cycle which was used for resin specimens. The glass fiber volume fraction was 50±2%.

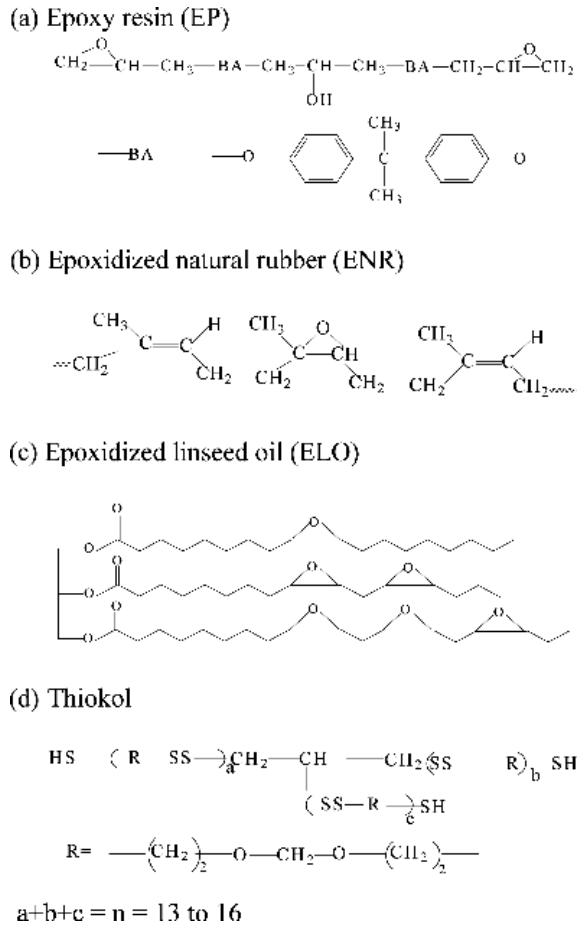

Figure 1. Structures of compounds.

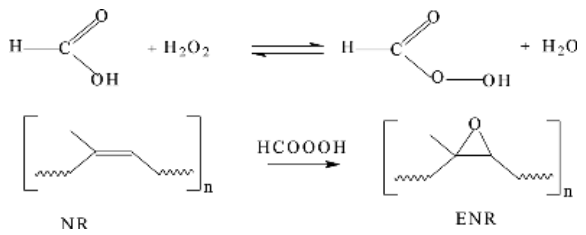

Figure 2. Epoxidation reaction of natural rubber.

Resin Fracture Toughness Test. The single edge notch bend (SENB) specimens (Figure 3) according to the ASTM (D5045-99) were used to test the fracture toughness (critical stress intensity factor, KIC). The notch tip was machined using a rotating saw, and the pre-crack of specimens was then generated by tapping on a fresh razor blade placed in the notch. The fracture toughness tests were conducted at a cross-head speed of 10 mm/min. The KIC value reported represents the average of at least five tests. The following eq. (1) was used to calculate the KIC:

$$KIC = \left(\frac{P_Q}{BW^{\frac{1}{2}}} \right) f(x) \tag{1}$$

With

$$f(x) = 6x^{\frac{1}{2}} \frac{[1.99 - x(1-x)(2.15 - 3.93x + 2.7x^2)]}{(1+2x)(1-x)^{\frac{3}{2}}}$$

where P_Q is a critical load for crack propagation (kN), B is the specimen thickness (cm), W is the specimen width (cm), $f(x)$ is the non-dimensional shape factor, a is the crack length (cm), and $x=a/W$.

Tensile Test. The tensile test was performed using the Instron 5582-100KN machine according to the ISO-527-1993. The specimen gauge length was 50±1 mm and the testing speed was set to 2 mm/min. The specimen dimension was 250×25×2.5 mm. Glass fiber reinforced plastic/epoxy tabs with a thickness of 1.5 mm were attached at both ends of the specimen by an adhesive. The values were taken from a mean of five specimens.

Mode-I Interlaminar Fracture Toughness Test. The mode I double cantilever beam (DCB) tests were carried out using the ASTM (D5528-01). The recommended specimen size is at least 150 mm long and 20 mm wide with an initial crack length (i.e. the length of the insert from the line) of 50 mm. Hinges of the same width as the specimen were attached to allow the application of a load. The load and dis-

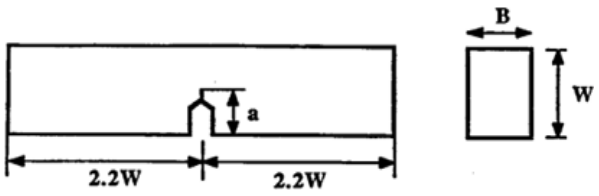

Figure 3. Schematic diagram of the KIC specimen.

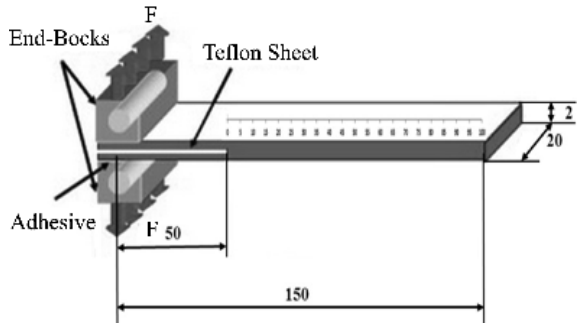

Figure 4. Geometry of DCB specimen (all dimensions in mm).

placement were then related to the delamination length as measured with a ruler on the specimen edge (Figure 4). The mode-I interlaminar fracture toughness GIC and GIP for each additive contents was calculated using the modified beam theory (MBT) method as follows:

$$GIC = \frac{3P_c\delta}{2b(a+|\Delta|)}\frac{F}{N} \quad (2)$$

$$GIP = \frac{3P_P\delta}{2b(a+|\Delta|)}\frac{F}{N} \quad (3)$$

where GIC is the fracture toughness at an initial crack stage corresponding to the first peak load in the force-displacement curves, GIP is the fracture toughness at the propagation stage that is taken from the plateau region of the R-curves, P_P is the applied load, C is the compliance corresponding to each crack length, a is the crack length, P_c is the initial maximum load, b is the specimen width, δ is a load point deflection, and Δ is an effective delamination extension to correct rotation of the DCB arms at the delamination front. In addition, N is the end-block correction factor, and F is a large displacement correction factor.

Morphology Analysis. The morphology was examined by both scanning electron microscopy (SEM) (Joel JSM 6360, Japan) and field emission scanning electron microscopy (FE-SEM) (S-4800, Hitachi), in which the fractured samples under mechanical analysis were sputter-coated with gold prior to the test.

Dielectric Measurement. The dielectric characteristics were examined using the basic free space measurement system consisting of a network analyzer (an Agilent PNA network analyzer), a sample holder, and two horn antennas with Agilent 8362B software. Two horn antennas were used as a transmitter and receiver, respectively, and the samples were placed between these two, as shown in Figure 5. The measurements were carried out in the frequency range of 4-8 GHz. The free-space reflection (S11) and transmission (S21) coefficients of the planar samples were measured after fixing the sample sheet at the reference plane. A mixture of the dielectric can also be found from the S11 and S21 parameter measurements. Complex permittivity, $\varepsilon^* = \varepsilon' - j\varepsilon''$, for each additive contents was calculated with respect to the frequency[22] with dielectric permittivity (ε') and loss factor (ε'').

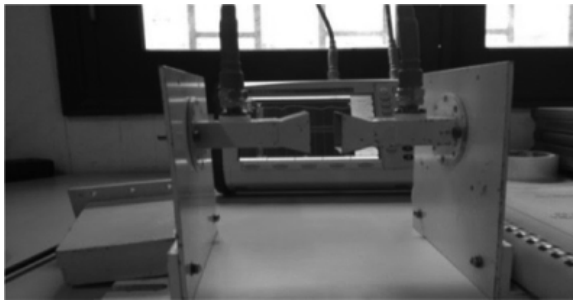

Figure 5. Photograph of the free space measurement system (PNA 8362B -Agilent USA).

Results and Discussion

Resin Fracture Toughness. Figure 6 shows the results of resin fracture toughness for neat epoxy, 5-20 phr ENR, 5-20 phr ELO, and 3-9 phr thiokol. The KIC values of epoxy resin improved significantly by adding each ENR, ELO, and thiokol. The addition of ENR, ELO, and thiokol imparts an increase in the KIC value up to an optimal content of 7, 9 and 5 phr, respectively. At 7 phr ENR, the fracture toughness improved by 56.9% from 0.65 to 1.02 MPa.m$^{1/2}$. At 9 phr ELO, the fracture toughness increased by 43.1% from 0.65 to 0.93 MPa.m$^{1/2}$, whereas at 5 phr thiokol, the fracture toughness increased by 80% from 0.65 to 1.17 MPa.m$^{1/2}$. No further increase was observed upon further loading of the additives. This may be attributed to the bigger size of rubber particles at higher concentrations. As noted from SEM pictures there is an increase in the size of particles for 15 phr ENR, 15 phr ELO

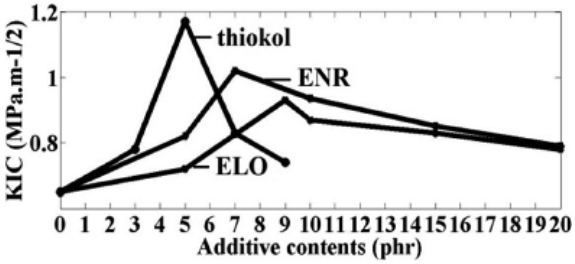

Figure 6. Effect of ENR, ELO, and thiokol contents on KIC of the epoxy resin.

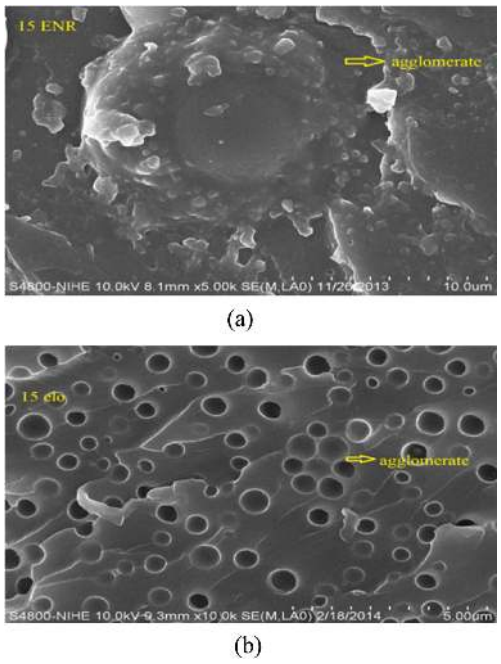

Figure 7. (a) ENR; (b) ELO aggregation in 15 phr blends.

blends (Figure 7). The large particles obtained at high additive content would deteriorate impact toughness as this would result in high stress intensity around the agglomerated rubber particles. The improvement in toughness attributed to additive particles that enhance the shear localization by acting as stress concentrators, crack deflections and crack pinning processes at obstacles, which was suggested to play an important role in toughening.[15,23] To better understand the toughening mechanism of the additives in the epoxy resin, the fractured surfaces of the specimens at zone ahead of the crack tip were observed by SEM. Figure 8(a) and (b) show that the fractured surface of the neat epoxy was smooth and glassy, which was the typical brittle fracture behavior of a thermosetting polymer. A smooth mirror-like surface with micro-flow lines was observed.

On the other hand, the fractured surface of the modified epoxy at 7 phr ENR, 9 phr ELO and 5 phr thiokol was rougher, and jagged multi-plane patterns appeared so that more energy was required. SEM of the ENR (Figure 8(c), (d)), ELO (Figure 8(e), (f)), and thiokol (Figure 8(g), (h))-modified systems revealed the presence of additive particles (ENR, ELO, and thiokol), which were dispersed throughout the epoxy matrix, i.e. they showed the presence of a two-phase morphological feature. The soft elastomeric phase in the case of ENR and thiokol was phase-separated from the hard epoxy matrix during the early stages of curing. The fractured surfaces of the most of the elastomer-toughened epoxy systems had a rigid

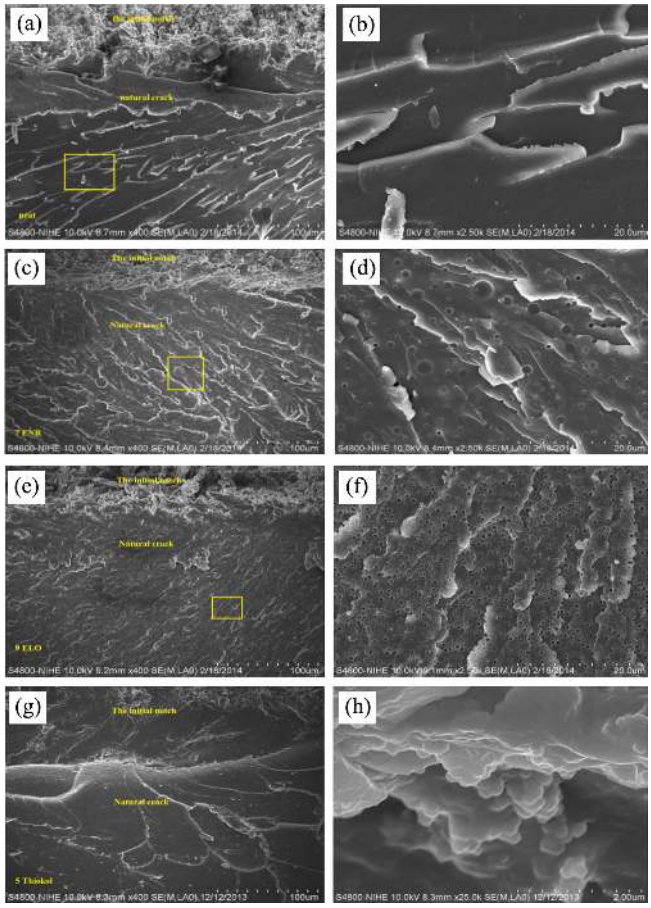

Figure 8. SEM images of the fractured surfaces of (a and b) neat epoxy, (e and f) 9 phr ELO, (c, d) 7 phr ENR, (g, h) 5 phr thiokol. The direction of crack propagation is from top to bottom.

continuous epoxy matrix with a dispersed rubbery phase as isolated particles. Different mechanisms, such as crazing, shear bonding and elastic deformation of the rubber particles have been proposed, and these mechanisms were believed to act alone or in the rubber particles, and these mechanisms were thought to act alone or in rubber-modified epoxy.[15,24]

Tensile Strength. The effect of additive contents on the large strain of the GF/EP was investigated up to their failure. Table 1 shows the tensile strength and Young's modulus for

Table 1. Tensile Strength and Young's Modulus for GF/EP at Different Contents of Additives

	Tensile strength (MPa)	Young's modulus (GPa)
Unmodified	187.94	6.792
7 phr ENR	185.60	6.708
9 phr ELO	182.34	6.625
5 phr thiokol	194.28	6.802

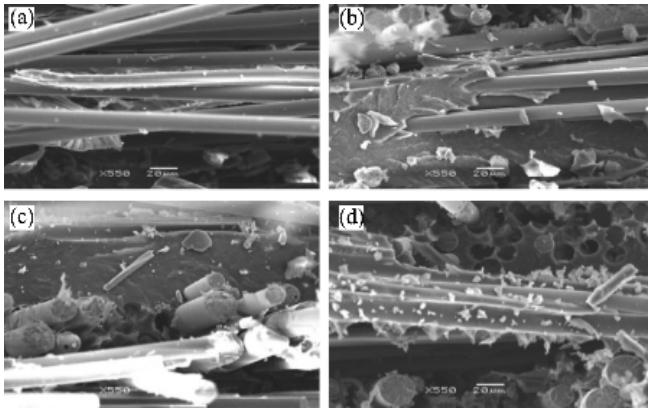

Figure 9. SEM images of the fractured surfaces of the GF/EP for the tensile testing specimens: (a) unmodified; (b) 5 phr thiokol; (c) 7 phr ENR; (d) 9 phr ELO.

GF/EP at different additive contents. For the modified composite, the tensile strength decreased slightly with the addition of 7 phr ENR and 9 phr ELO. These can be attributed to the fact that the modulus of ENR and ELO is much lower than that of the epoxy matrix as well as glass fiber. In addition, low modulus ENR and ELO particles act as stress concentrators and decrease the yield strength.[25] Although there is a tendency to increase tensile strength for 5 phr thiokol modified GF/EP, the increase was no significant.

The Young's modulus, determined from the typical stress-strain curve, showed little decrease for composites modified with 7 phr ENR, and 9 phr ELO. The Young's modulus with addition of 5 phr thiokol slightly increased.

SEM clearly showed the broken fiber pull-out at the fractured surface of the glass fiber as well as the fiber breakage for both the unmodified composite and modified composite, as shown in Figure 9(a), (b), (c) and (d). The most distinct feature of the fractured surface with the addition of elastomers of thiokol and ENR was the extensive matrix deformation between the clean fiber and matrix. Although there was extensive matrix deformation, the tensile strength of the GF/EP was not strongly affected by the addition of the additives. The addition of additives which are characterized by large surface areas per unit gram plays an important role in determining the strength of the interface. The addition of additives leading to the number of adhesively jointed points with glass fibers was very low, which had no effect on tensile strength of the GF/EP.

Mode-I Interlaminar Fracture Toughness Test. The delamination resistance curves (R-curves) are drawn between the crack length (a) and the corresponding fracture toughness, as shown in Figure 10. The GIC value corresponding to the

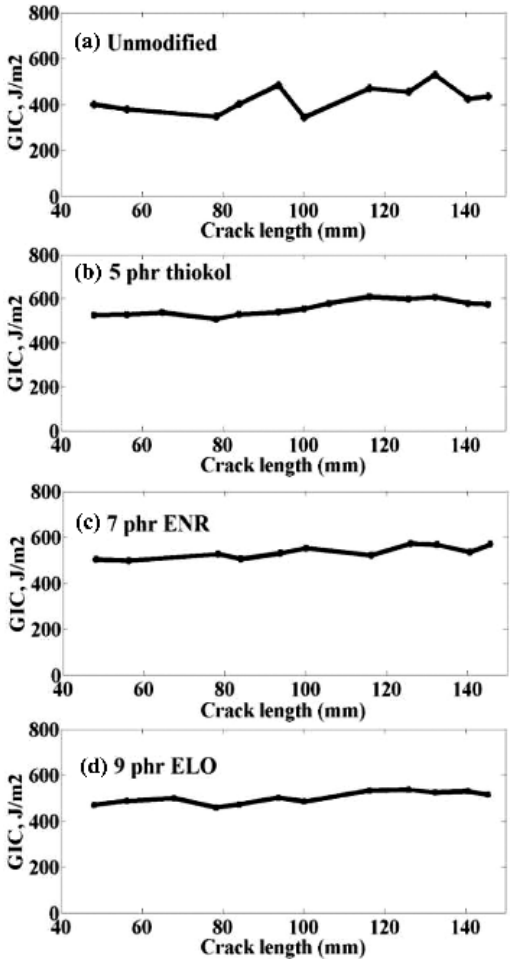

Figure 10. Typical delamination resistance (R-curves) of the GF/EP with various additive contents: (a) unmodified; (b) 5 phr thiokol; (c) 7 phr ENR; (d) 9 phr ELO.

first crack initiation was determined from the load point at which the initiation of delamination is observed at the microscopic level on the specimen edge. The crack growth rate of the unmodified GF/EP propagates smoothly in wide steps as a result of the relatively low tenacity of the polymeric phase with glass fibers. On the other hand, the crack of the GF/EP with 5 phr thiokol, 7 phr ENR and 9 phr ELO was deflected and pinned gradually by the reinforcing obstacles so that more energy was required, resulting in higher fracture toughness. The delamination initiation (GIC) values were reported throughout this investigation corresponding to first peak load in the load-crack opening displacement curves, whereas the delamination propagation (GIP) values were taken from the plateau region of the R-curves.[26]

The mode-I interlaminar fracture toughness of the GF/EP was determined using the DCB test, in which the curves of the

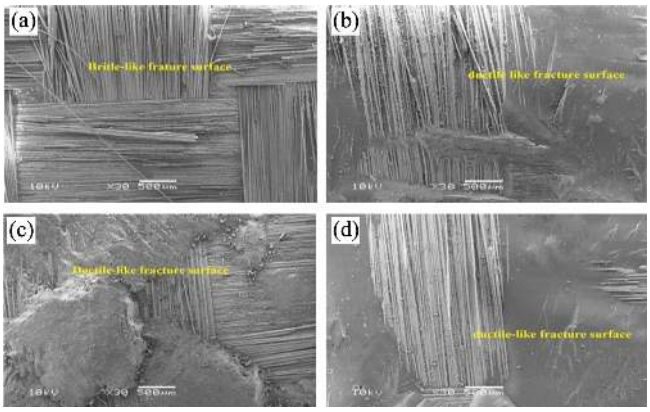

Figure 11. SEM images of the fractured surface of GF/EP for the fracture toughness testing specimen: (a) unmodified; (b) 5 phr thiokol; (c) 7 phr ENR; (d) 9 phr ELO.

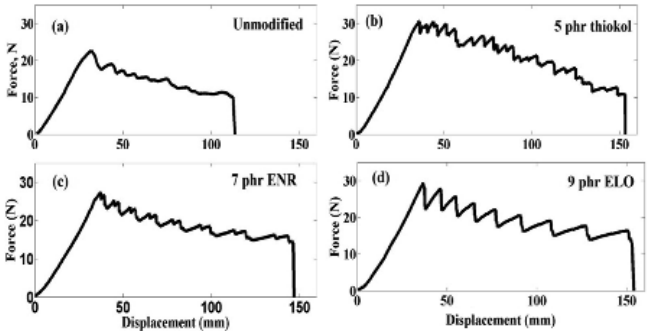

Figure 12. Typical force-displacement curves of the (a) unmodified; (b) 5 phr thiokol; (c) 7 phr ENR; (d) 9 phr ELO.

applied load *vs*. displacement were recorded. Figure 11 showed that the force increased linearly until the maximum force value was reached, then decreased gradually in the manner of a zigzag shape (stick-slip) in the propagation stages.

For the modified composite, both the displacement and force values in Figure 12 were higher than those of the unmodified composite. The crack was suggested to propagate more stably and gradually as a result of the relatively high tenaciousness of the epoxy modified with the elastomer. Moreover, the mode-I interlaminar fracture toughness values were calculated using the MBT method, as shown in Figure 13.

A significantly increased in the mode-I interlaminar fracture toughness with the modified epoxy resin additives was observed. At 5 phr thiokol, 7 phr ENR and 9 phr ELO content, the crack initiation (GIC) increased by 30.3, 26.9 and 17.6%, respectively, and the GIP values also increased by 32.7, 26.9 and 18.3%, respectively, compared to the unmodified composite. The presence of thiokol, ENR, and ELO in GF/EP acted as an obstacle reinforcement that deflected, pinned and

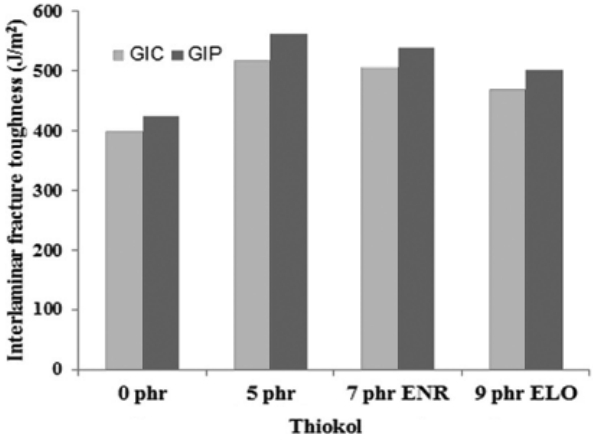

Figure 13. Initiation (GIC) and propagation (GIP) fracture toughness in mode I of the GF/EP composite with various contents of additives.

delayed the crack propagations, so more energy was required. The major energy absorption mechanism in the composite, which are: crack deflection, debonding between the fiber and resin, pull-out (extraction of the fibers from the resin), and fiber-bridging mechanism.[13,27] In general, a number of mechanisms contribute to the fracture toughness, and it is often very difficult to determine the dominant mechanism. SEM of the fractured surfaces of specimens revealed clear damage in the interfacial region in the composite. For the unmodified composite (Figure 11(a)), the fractured surfaces were mostly smooth and glassy due to brittle failure. Therefore, the energy required for the interlaminar delamination failure was low. In contrast, the additives strongly affected the mode-I interlaminar fracture toughness, as shown in Figure 11(b), (c), and (d). The fractured surface of the additive-modified composite had a rougher surface and was tougher than those of the unmodified composite. Therefore, more energy was required, resulting in higher fracture toughness.

The dielectric property, which is a measure of the polarizability of a material when subjected to an electric field, is an important factor in defining the physical and chemical properties related to the storage and energy loss in various materials. The permittivity (ε), which is also known as a material's dielectric constant, describes the interaction of a material with an electric field. The dielectric constant is equivalent to the relative permittivity or the absolute permittivity (ε) relative to the permittivity of free space. The real part of the permittivity (ε') is a measure of how much energy from an external electric field is stored in a material. The imaginary part of the permittivity (ε'') is called the loss factor and is a measure of how

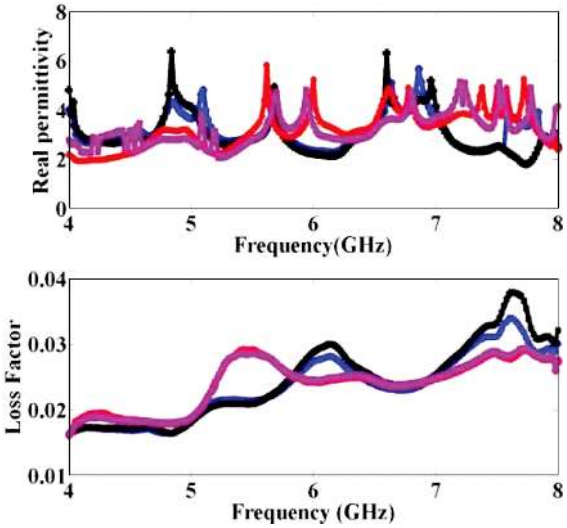

Figure 14. Variations of the real permittivity (ε') and loss factor (ε'') as a function of frequencys for GF/EP with unmodified (purple line), 5 phr thiokol (red line), 9 phr ELO (blue line), and 7 phr ENR (black line).

Table 2. Dielectric Properties of the Modified and Unmodified GF/EP

Materials	Dielectric properties	
	ε'	ε''
Unmodified	3.178	0.0240
5 phr thiokol	3.457	0.0239
7 phr ENR	3.791	0.0243
9 phr ELO	3.625	0.0235

the dissipative or loss of a material is to an external electric field.

Figure 14 shows the measured permittivity of the specimens, in which the ENR, ELO, and thiokol-modified GF/EP have a similar real permittivity and loss factor line compared to the unmodified GF/EP, indicating that the thiokol, ENR, and ELO-modified GF/EP had no effect on the external electric field compared to the unmodified GF/EP. The average results of the dielectric properties measurements were calculated from 4 GHz until 8 GHz, and are presented in Table 2. The average real part of the permittivity (ε') of the unmodified GF/EP, and GF/EP modified with 5 phr thiokol, 7 phr ENR, 9 phr ELO were 3.178, 3.457, 3.791, and 3.625. The average real part of the permittivity (ε') with the addition of thiokol, ENR, and ELO increased slightly. The small values of the real part of the permittivity showed that there was no more external electric field stored in the material, which agrees with the loss factor. The loss factor of 5 phr thiokol, 7 phr ENR, 9 phr ELO modified and unmodified GF/EP were 0.0239, 0.0243, 0.0235, and 0.024, respectively, suggesting little external electric field loss and confirming that thiokol, ENR, and ELO had no added effect on the dielectric properties of the GF/EP.

Conclusions

By introducing a novel GF/EP modified with thiokol, ENR, and ELO, we examined the effects of additives on the mechanical and dielectric properties of GF/EP in this study. With the addition of 5 phr thiokol, 7 phr ENR, and 9 phr ELO, the fracture toughness of the epoxy resin increased by 80.0, 56.9 and 43.1%, respectively. The mode-I interlaminar fracture toughness of GF/EP containing 5 phr thiokol, 7 phr ENR and 9 phr ELO contents for the GIC increased by 30.3, 26.9 and 17.6%, respectively, and for the crack propagation, the GIP values also increased by 32.7, 26.9 and 18.3%, respectively, compared to the unmodified composite. The dielectric properties obtained from the free space method for frequencys 4-8 GHz at room temperature of 28 ºC showed that all these additives had no added effect on the dielectric properties of the GF/EP.

The GF/EP modified with 5 phr thiokol showed the best mechanical properties compared to the 7 phr ENR and 9 phr ELO modified GF/EP.

References

1. J. H. Chen, E. Schulz, J. Bohse, and G. Hinrichsen, *Compos.: A,* **30,** 747 (1999).
2. A. C. Garg and Y. W. Mai, *Compos. Sci. Technol.*, **31**, 179 (1988).
3. T. Adachi, M. Osaki, W. Araki, and S. C. Kwon, *Acta Mater.*, **56**, 2101 (2008).
4. S. Y. Fu, X. Q. Feng, B. Lauke, and Y. W. Mai, *Compos.: B*, **39**, 933 (2008).
5. R. Bagheri, B. T. Marouf, and R. A. Pearson, *J. Macromol. Sci. C: Polym. Rev.*, **49**, 201 (2009).
6. M. Arai, Y. Noro, K.-I. Sugimoto, and M. Endo, *Compos. Sci. Technol.*, **68**, 516 (2008).
7. N. A. Siddiqui, R. S. C. Woo, J. K. Kim, C. C. K. Leung, and A. Munir, *Compos.: A*, **38**, 449 (2007).
8. M. H. Gabr, M. A. Elrahman, K. Okubo, and T. Fujii, *Compos. Struct.*, **92**, 1999 (2010).
9. B. Ashrafi, J. Guan, V. Mirjalili, Y. Zhang, L. Chun, P. Hubert, B. Simard, C. T. Kingston, O. Bourne, and A. Johnston, *Compos. Sci. Technol.,* **71,** 1569 (2011).
10. Y. Xu and S. V. Hoa. *Compos. Sci. Technol.*, **68**, 854 (2008).
11. H. Y. Liu, G. T. Wang, Y. W. Mai, and Y. Zeng, *Compos.: B*, **42**, 2170 (2011).
12. M. Abadyan, V. Khademi, R. Bagheri, H. Haddadpour, M. A.

Kouchakzadeh, and M. Farsadi, *Mater. Des.*, **30**, 1976 (2009).
13. M. H. Gabr, M. A. Elrahman, K. Okubo, and T. Fujii, *Compos.: A*, **41**, 1263 (2010).
14. S. Balakrishnan, P. R. Start, D. Raghavan, and S. D. Hudson, *Polymer*, **46**, 11255 (2005).
15. R. Thomas, Y. M. Ding, Y. L. He, L. Yang, P. Moldenaers, W. M. Yang, T. Czigany, and S. Thomas, *Polymer*, **49**, 278 (2008).
16. G. Tripathi and D. Srivastava, *Mater. Sci. Eng. A*, **496**, 483 (2008).
17. N. Chikhi, S. Fellahi, and M. Bakar, *Eur. Polym. J.*, **38**, 251 (2002).
18. M. Abadyan, R. Bagheri, H. Haddadpour, and P. Motamedi, *Mater. Des.*, **30**, 3048 (2009).
19. M. Abadyan, R. Bagheri, M. A. Kouchakzadeh, and S. A. Hosseini Kordkheili, *Mater. Des.*, **32**, 2900 (2011).
20. J. K. Kim, C. Baillie, J. Poh, and Y. W. Mai, *Compos. Sci. Technol*., **43**, 283 (1992).
21. I. S. Seo, W. S. Chin, and D. G. Lee, *Compos. Struct*., **66**, 533 (2004).
22. D. K. Ghodgaonkar, V. V. Varadan, and V. K. Varadan, *IEEE Trans. Instrum. Meas.*, **37**, 789 (1989).
23. G. Gkikas, N. M. Barkoula, and A. S. Paipetis, *Compos.: B*, **43**, 2697 (2012).
24. V. D. Ramos, H. M. da Costa, V. L. P. Soares, and R. S. V. Nascimento, *Polym. Test.*, **24**, 387 (2005).
25. M. Abadyan, V. Khademi, R. Bagheri, H. Haddadpour, M. A. Kouchakzadeh, and M. Farsadi, *Compos. Mater. Des*., **30**, 1976 (2009).
26. R. Velmurugan and S. Solaimurugan, *Compos. Sci. Technol.*, **67**, 61 (2007).
27. D. W. Y. Wong, L. Lin, P. T. McGrail, T. Peijs, and P. J. Hogg, *Compos.: A*, **41**, 759 (2010).